Central European Journal of Energetic Materials, **2013**, *10*(1), 69-85
ISSN 1733-7178

Use of a Hot-Spot Model to Describe the Influence of Particle Size and Distance on Combustion in a Cloud

Stefan KELZENBERG*, Sebastian KNAPP, Volker WEISER and Norbert EISENREICH

Fraunhofer Institut für Chemische Technologie ICT, Pfinztal, Germany
**E-mail: stefan.kelzenberg@ict.fraunhofer.de*

Abstract: The combustion of particles in a cloud can be very different from single particle combustion. In addition to the size of the particles, the number density of particles or the mean distance between the particles plays an important role. Experiments show that if the distance between the particles in a cloud is large enough, particles burn in a similar manner to single particles. However below a certain distance, particles form a common flame front. In a parametric study, a hot-spot model is used to simulate the two burning regimes and to find the critical parameters for the transition between them. The results are discussed with reference to the combustion of metalized, gelled and solid propellants and dust explosions.

Keywords: combustion, particles, hot-spot-model

Introduction

The ignition, combustion and detonation of powders have recently gained increased importance because of investigations of the influences of nano-particles dispersed in reactive gases [1-14]. These related phenomena and their relevant parameters strongly depend on the particle size and on the particle morphology, as well as on the distribution of the particles in a particle cloud. Of especial importance is the ratio of distance to diameter, which was proved in detail 50 years ago for liquid fuels [15-23] when the liquid fuel droplets were assumed to behave in a similar manner to bare (without oxide layers) metallic particles [24-26]. The current interest is based on various types of applications.

These include safety problems on storing, handling and processing in industry. Especially severe dust explosions might be expected [2-7] and could include deflagration to detonation transitions (DDT). In solid rocket propellants, metal particles increase the performance and nano-particles enable a more flexible design, their conversion occurring predominantly in the hot gas phase [27-33]. In explosion and detonation research nano-particles might substantially enhance blast due to reactions with entrained air in the expanding fumes [34-37]. The oxidation behavior of nano-particles is essentially dependent on the particle size [14], with strongly increased conversion rates [38-42] and could explain some of the observed phenomena, but the behaviour of nano-particles in clouds might also deviate from that of larger particles [2].

Consequently modelling is of particular interest and there have been some preliminary approaches with complex structures, which could describe particle ignition and the propagation of reaction fronts in porous energetic materials [43-46]. These use only the heat flow equation with simplified reaction mechanisms. More developed approaches also include the reaction and diffusion of reactants. This Hot-Spot modelling approach is suitable for theoretical multi-droplet- or cloud-investigations [47, 48]. The model is substantially simplified and includes only the heat flow and diffusion equations in 3 dimensions for some species and a simple (0^{th} order reaction) or even a complex chemical reaction model. However until now, no detailed parametric studies have been performed. The intensive use of the Hot Spot model qualitative investigation will be initiated in this paper for multi-droplets in an oxidizing atmosphere. Primarily, the influence of the fuel droplet distance to diameter ratio is studied using normalized parameters and kinetic data and compared with the results from a quasi steady-state model [49-51]. In particular, this investigation will be test whether the results can qualitatively reproduce the different combustion modes found in the transition from single droplet combustion to group combustion and sheet combustion in a particle cloud.

Quasi steady-state theory for multi-particle combustion

The ignition and combustion of particles – with the fuel in the liquid/solid phase and the oxidizer in the gas phase or vice versa – has been widely investigated for liquid droplets, metal and coal particles. The basic differential equations were summarized, for example, by Williams [49], Kuo [50] and Sirignano [51]. The solutions and the comparison with experimental results, and theoretical refinements of the description is still on-going research, actually

mainly carried out under microgravity (*e.g.* [51]).

These diffusion controlled, heterogeneous reactions are often described using a quasi steady-state approximation, where only transport phenomena are used. The analytical procedure includes a chemical reaction between the fuel and the oxidizer, the heat transfer equation and the diffusion equations for a gaseous oxidizer (fuel) and an evaporating fuel (oxidizer) droplet, which can be represented by a Shvab-Zeldovich variable for one equation. The simplified quasi steady-state theory is briefly outlined here (see [15, 49-51]).

It proceeds from the assumption that a vaporizing or burning droplet generates a flow field quasi-independent of time in the gas phase.

From the continuity equation

$$\frac{\partial \rho_g}{\partial t} + \frac{1}{r^2}\frac{\partial}{\partial r}(r^2 \rho_g v_g) = 0 \tag{1}$$

follows for a quasi steady-state: $r^2 \rho_g v_g = const = a$, ρ_g gas density, v_g gas velocity.

Profiles of the temperature and the reactants (ambient mass fractions: Y_{OX} oxidiser, Y_F fuel and Y_P reaction product) in the gas are described by the equation:

$$\frac{d}{dr}[(r^2 \rho_g v_g)(c_p T + Q_O Y_{OX}) - r^2 \rho_g D \frac{d}{dr}(c_p T + Q_O Y_{OX})] = 0 \tag{2}$$

and similar equations arise where Y_{OX} is substituted by Y_F or Y_P, with boundary conditions *e.g.*: $Y_F = 0$, $Y_{OX} = Y_{OX,\infty}$, $Y_P = 0$ (Y mass fraction) and $T = T_\infty$ for $r = \infty$ and $Y_{OX} = 0$, $Y_F = 1$ and $T = T_S$ for $r = d/2$ (droplet surface) and $(\lambda dT/dr)_g = \rho_g v_g L + (\lambda dT/dr)_l + Q_R$ for $r = d/2$; λ heat conductivity, Q_O reaction enthalpy related to the oxidizer, L heat of vaporization, β stoichiometric fuel to oxidizer mass ratio.

The solution of equation (2) is (C_1 and C_2 are integration constants):

$$c_P T + Q_O Y_{OX} = C_1 + C_2 e^{-\frac{a}{r \rho_g D}} \tag{3}$$

$$\rho_g v_g \frac{d}{2} = \rho_g D \ln(1 + B) \tag{4}$$

B is the Spalding transfer number:

$$B = \frac{\beta Q_O Y_{OX} + c_{p,g}(T_\infty - T_S)}{L + \lambda (dT/dr)_l + Q_R} \tag{5}$$

Figure 1 demonstrates the kind of results which can be expected from calculations with the theory described above. Some of them have been very successful, but, for example, the stand-off distance of the flame is given as too large. One problem is to find reasonable values for the material parameters; therefore the results have often been given in arbitrary units or as dimensionless quantities.

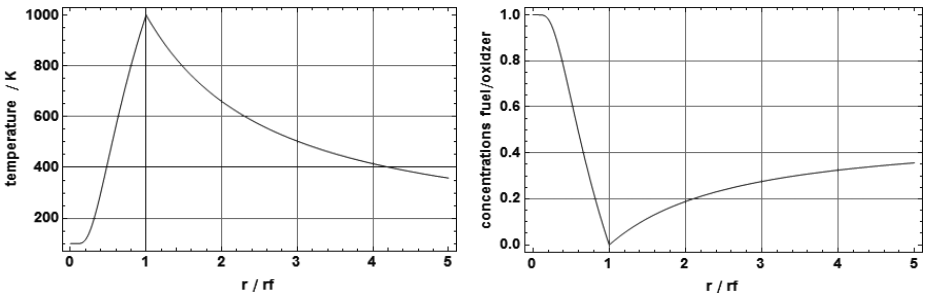

Figure 1. Temperature and concentration profiles according to quasi steady-state theory for a single droplet (r_f flame radius, d droplet diameter, $r_f/d = 50$).

For more than one droplet the differential equation can be written as:

$$\sum_i \frac{1}{(r-r_i)^2} \frac{\partial}{\partial r} \left(b \cdot F[r] - \frac{1}{\sum_i \frac{1}{(r-r_i)^2}} \frac{\partial}{\partial r} F[r] \right) = 0 \tag{6}$$

with the general solution:

$$F[r] = C_1 + \frac{C_2}{b} \mathrm{Exp}\left[- \frac{b}{\sum_i \sqrt{(r-r_i)^2}} \right] \tag{7}$$

F stands for T, Y_{OX}, Y_F or Y_P, and the parameter b is defined for T as $b = \frac{\lambda}{\dot{m}'' \cdot c_p}$, and for Y as $b = \frac{\rho D}{\dot{m}''}$. A more detailed description is given in reference [48]. The examples in Figure 2 show the concentration profiles of three droplets with different distances. The position of the flame has fuel and oxidizer concentrations

equal to zero. For short distances there is an overlap of the fuel concentration and the droplets are enclosed in a common flame.

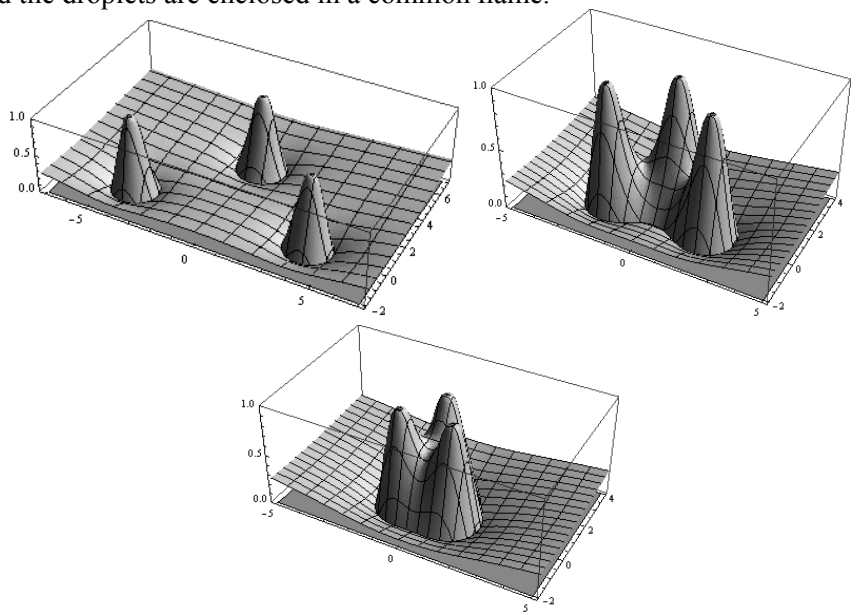

Figure 2. Concentration profiles for three droplets at different distances ($r_f/d = 5$, $l/d \approx 30$, $l/d \approx 13$, $l/d \approx 10$).

The Hot-Spot-Model for fuel droplets in an oxidizing atmosphere

Hot-Spot-Modelling of the ignition and combustion of a multi-droplet cloud in an oxidizing atmosphere uses the heat flow equation simultaneously with the mass transfer equation and with the Green's function approach in 3 dimensions. It includes a 2nd order reaction of a fuel with an oxidizer which converts these to a reaction product and generates heat according to the heat of combustion. For such processes, the related partial differential equations have to be solved for temperature and for at least 3 species c_i. The transport coefficients, heat conductivity and species diffusivity are assumed to be independent of temperature and species concentrations. These simplifications, however, enable a 3-dimensional calculation to be performed with substantially more than 10^6 lattice points.

The fuel droplets or particles are assumed to be Gaussians and the oxidizer

complementarily fills the residual space. The droplets can be distributed arbitrarily or regularly. These Gaussians spread out by the diffusion equation, therefore it is only realistic for supercritical fluids [52], but a good approximation is obtained for qualitative approaches. An instantaneously inserted temperature profile, mainly a Gaussian, initiates the reaction in the droplet cloud with the surrounding oxidizing atmosphere.

This means that heat and species are generated and consumed at the combustion front and distributed in the material and the burn-out zone.

$$\rho c_p \frac{\partial T[\vec{x},t]}{\partial t} - \lambda \cdot \Delta T[\vec{x},t] = \dot{Q}[\vec{x},t] \tag{8}$$

$$\frac{\partial c_i[\vec{x},t]}{\partial t} - D_i \Delta c_i[\vec{x},t] = \dot{c}_i[\vec{x},t] \tag{9}$$

where ρ is the density, c_p the specific heat capacity and λ the heat conductivity, D_i the diffusion coefficient for the i-th species and $c_i[\vec{x}, t]$ the concentration of component i. The equations describe the propagation of the scalar temperature field and the species fields in space and time in terms of the physical properties of the material and of the source terms on the right hand side. The source terms comprise the chemical reactions, and the related heat and species generation and consumption.

In the case of the combustion of a fuel droplet (oxidation), the chemical reaction is exothermic, and consequently heat release occurs. The source term of the energy release by the chemical reaction is given for a general reaction scheme by:

$$\dot{Q}_{react}[\vec{x},t] = \sum_i q_i \frac{\partial c_i[\vec{x},t]}{\partial t} \tag{10}$$

whereas q_i are the heats of reaction. The rates of reaction are given by

$$\frac{\partial c_i[\vec{x},t]}{\partial t} = -\sum k_{i,j} f[c_i, c_j] \tag{11}$$

with the rate constants $k_{i,j}$ given by the Arrhenius equation:

$$k_{i,j}[T] = Z_{i,j} e^{-\frac{E_{A,i,j}}{RT[\vec{x},t]}} \tag{12}$$

Here, $Z_{i,j}$ is the pre-exponential factor, R the universal gas constant, T the temperature and $E_{A,i,j}$ the activation energy. The Arrhenius equation gives the dependence of the rate constant $k_{i,j}$ of the chemical reactions on the temperature

T and the activation energies $E_{A,i,j}$.

The function $f[c_i,c_j]$ in equation (11) depends on the reaction scheme to be modelled. In the case of a chemical reaction of a fuel with an oxidizer generating the heat of reaction q_{reac}, such as $A + B \rightarrow C$ (i = A, B, C), a second order reaction is assumed. The heat output of the chemical reaction and therefore the source term for the chemical reaction energy release in the equation of heat transfer is given by:

$$\frac{dc_A[\vec{x},t]}{dt} = -k[T_1[\vec{x},t]]c_A[\vec{x},t]c_B[\vec{x},t] \tag{13}$$

$$\frac{dc_B[\vec{x},t]}{dt} = -k[T_1[\vec{x},t]]c_A[\vec{x},t]c_B[\vec{x},t] \tag{14}$$

$$\frac{dc_C[\vec{x},t]}{dt} = -\frac{dc_A[\vec{x},t]}{dt} = -\frac{dc_B[\vec{x},t]}{dt} \tag{15}$$

$$\dot{Q}_{reac}[\vec{x},t] = q_{reac} Z_{A,B} e^{-\frac{E_A}{RT_1[\vec{x},t]}} c_A[\vec{x},t]c_B[\vec{x},t] \tag{16}$$

Without interdiffusion, both components, fuel and oxidizer, would develop at all positions $\vec{x}$ according to the solution of equation (11) for the proposed case of a 2nd order reaction:

$$c_A[\vec{x},t] = \frac{c_{A0} - c_{B0}}{1 - c_{B0}/c_{A0} \cdot e^{(c_{B0}-c_{A0})k\cdot t}} \tag{17}$$

$$c_B[\vec{x},t] = \frac{c_{B0} - c_{A0}}{1 - c_{A0}/c_{B0} \cdot e^{(c_{A0}-c_{B0})k\cdot t}} \tag{18}$$

$$c_C[\vec{x},t] = 1 - c_A[\vec{x},t] = 1 - c_B[\vec{x},t] \tag{19}$$

To start the combustion process of a fuel droplet and oxidizer mixture it must be ignited. In the heat transfer equation a second source term on the right hand side must provide an energy input at a defined point in time and space. This is called a Hot-Spot. For example, it can be described by a 3D-Gaussian-function at position (x_0, y_0, z_0):

$$\dot{Q}_{hs}[\vec{x},0] = \frac{Q_0}{(2\pi)^{3/2}\sigma_x\sigma_y\sigma_z} \cdot e^{-\left(\frac{(x-x_0)^2}{2\sigma_x^2} + \frac{(y-y_0)^2}{2\sigma_y^2} + \frac{(z-z_0)^2}{2\sigma_z^2}\right)} \tag{20}$$

Including the initiating hot spot at t_0 and the heat of reaction in the equation of heat transfer, results in:

$$\rho c_p \frac{\partial T[\vec{x},t]}{\partial t} - \lambda \cdot \Delta T[\vec{x},t] = \dot{Q}_{hs}[\vec{x},t] + \dot{Q}_{reac}[\vec{x}',t] \tag{21}$$

The fuel droplets are introduced by an ensemble of *n* Gaussians:

$$c_{1,A}[\vec{x},t] = \sum_{i=1}^{n} \left(\frac{1}{(2\pi)^{3/2} \sigma_x \sigma_y \sigma_z} \cdot e^{-\left(\frac{(x'-x_i)^2}{2\sigma_x^2} + \frac{(y'-y_i)^2}{2\sigma_y^2} + \frac{(z'-z_i)^2}{2\sigma_z^2} \right)} \right) \tag{22}$$

Without a chemical reaction ($\dot{Q}_{reac}[\vec{x}', t]$) the problem can be solved analytically and several analytical and numerical methods are known [49]. However the non-linearity of the Arrhenius term prevents an analytical solution. Therefore, only a numerical method can be applied in this case. In order to avoid the current, cumbersome methods of numerically solving differential equations, the method of Green`s function is used, where a numerical integration is performed. This is a faster and a more stable process and enables complex geometries generated by the reaction of the individual particles to be involved. If the appropriate Green's function for the homogeneous problem is known, it only has to be convolved with the source term of the differential equation in the case of infinite space.

The Green's function in infinite space for the differential equation above in three dimensions is a Gaussian-like function ($\kappa = \lambda/(c_p\rho)$) [53].

$$G_U[\vec{x}-\vec{x}', t-t'] = \left(\frac{1}{4\pi\kappa(t-t')} \right)^{3/2} \cdot e^{-\frac{(\vec{x}-\vec{x}')^2}{4\kappa(t-t')}} \tag{23}$$

For the initiating Hot Spot, the solution reads for infinite space and no reaction:

$$T[\vec{x},t] = \int G_U[\vec{x}-\vec{x}', t-t'] \cdot \frac{\dot{Q}_{hs}[\vec{x},t]}{\rho c_p} \cdot d\vec{x}' \cdot dt' \tag{24}$$

and for the fuel particles:

$$c_{i,A}[\vec{x},t] = \int_0^t \int_{-\infty}^{\infty} \frac{1}{\left(4\pi D(t-t')\right)^{3/2}} \cdot e^{-\frac{(\vec{x}-\vec{x}')^2}{4D(t-t')}} \cdot c_{i,A}[\vec{x}',t] d\vec{x}' dt \tag{25}$$

With chemical reaction and heat release:

$$T(\vec{x},t) = \int_0^t \int_{-\infty}^{\infty} \frac{1}{\left(4\pi\kappa(t-t')\right)^{3/2}} \cdot e^{-\frac{(\vec{x}-\vec{x}')^2}{4\kappa(t-t')}} \cdot \left(\dot{Q}_{hs}[\vec{x}',t] + \dot{Q}_{reac}[\vec{x}',t] \right) d\vec{x}' dt \tag{26}$$

The profiles of oxidizer, fuel and reaction product proceed in an analogous way:

$$c_i(\vec{x},t)=\int_0^t\int_{-\infty}^{\infty}\frac{1}{\left(4\pi D(t-t')\right)^{3/2}}\cdot e^{-\frac{(\vec{x}-\vec{x}')^2}{4D(t-t')}}\cdot \dot{c}_i[\vec{x}',t]d\vec{x}'dt \tag{27}$$

The numerical solution starts with the initial temperature profile of the Hot Spot (see equation (20)) and the fuel/oxidizer distributions (see equation (22)). It then uses time increments Δt to obtain, at these stages, the development of the species concentrations and the related heat for all positions, and the related temperatures from equations (16)-(19), and sums up these values to give initial profiles. Therefore the numerical solution uses an iteration algorithm mainly consisting of three steps. The first step generates the initial temperature and species profiles, as described above, resulting from the initially given igniting hot spot (equation (28)) and the *n* particles of both types, the fuel A (equation (29)) approximated by 3D-Gaussians and the oxidizer B as a background (equation (30)):

$$T_1[\vec{x},t]=\frac{1}{\rho c_p}\dot{Q}_{hs}[\vec{x},t] \tag{28}$$

$$c_{1,A}[\vec{x},t]=\sum_{i=1}^{n}\left(\frac{1}{(2\pi)^{3/2}\sigma_x\sigma_y\sigma_z}\cdot e^{-\left(\frac{(x'-x_i)^2}{2\sigma_x^2}+\frac{(y'-y_i)^2}{2\sigma_y^2}+\frac{(z'-z_i)^2}{2\sigma_z^2}\right)}\right) \tag{29}$$

$$c_{1,B}[\vec{x},t]=1-c_{1,A}[\vec{x},t] \tag{30}$$

$$c_{1,C}[\vec{x},t]=0 \tag{31}$$

In the second step, the progress of the chemical reaction, equations (26) and (27), for a small time increment Δt is calculated generating:

$$T_2(\vec{x},t)=T_1[\vec{x},t]+\frac{q_{reac}}{\rho c_p}\cdot k\left[T_1[\vec{x},t]\right]c_{1,A}[\vec{x},t]c_{1,B}[\vec{x},t]\cdot\Delta t \tag{32}$$

with:

$$c_{2,A}[\vec{x},t]=c_{1,A}[\vec{x},t]-k\left[T_1[\vec{x},t]\right]c_{1,A}[\vec{x},t]c_{1,B}[\vec{x},t]\cdot\Delta t \tag{33}$$

$$c_{2,B}[\vec{x},t]=c_{1,B}[\vec{x},t]-k\left[T_1[\vec{x},t]\right]c_{1,A}[\vec{x},t]c_{1,B}[\vec{x},t]\cdot\Delta t \tag{34}$$

$$c_{2,C}[\vec{x},t]=c_{1,C}[\vec{x},t]+k\left[T_1[\vec{x},t]\right]c_{1,A}[\vec{x},t]c_{1,B}[\vec{x},t]\cdot\Delta t \tag{35}$$

These temperature and species profiles are assumed to be instantaneously inserted, each being multiplied by the Dirac Delta function $\delta(t)$. The third step is to calculate the solution of the transport equations. This calculates the heat and mass diffusion for that same time increment Δt by convolution of the related profiles and the Green's functions.

$$T_3[\vec{x},t] = \int\int\left(\frac{1}{4\pi\kappa(t-t')}\right)^{3/2} \cdot e^{-\frac{(\vec{x}-\vec{x}')^2}{4\kappa(t-t')}} \cdot T_2[\vec{x}',t'] \cdot \delta(t') \cdot d\vec{x}' \cdot dt' \tag{36}$$

$$c_{3,i}[\vec{x},t] = \int\int\left(\frac{1}{4\pi D_i(t-t')}\right)^{3/2} \cdot e^{-\frac{(\vec{x}-\vec{x}')^2}{4D_i(t-t')}} \cdot c_{2,i}[\vec{x},t'] \cdot \delta(t') \cdot d\vec{x}' \cdot dt' \tag{37}$$

The integral, via dt', results in the integrand itself, because of the Dirac Delta function. The numerical procedure *e.g.* 3D Gaussian Quadrature [54], performs the spatial integral on a 3D lattice. In case of steep gradients and short time intervals, and the correlated squares of the lattice node distances Δx^2, the Green's function is of small width and strongly reduces computing time because of the reduction of the integral intervals to those sections where the Green's function $G_{\underline{U}} \neq 0$. The spatial integrals in principle reach over infinite space. According to the boundary conditions of the limited sizes of a real sample, the energy (temperature) and species will be reflected at the boundaries of the sample by the use of mirror sources beyond the boundaries. The integral then only extends over the sample dimensions. This approach avoids the use of boundary conditions in the Green's function, normally needed for the Green's function in limited space. In the case of fast reactions and steep profiles of temperatures and species, the width of G_U is small compared with the size of the included space at adequate $\Delta x^2/\Delta t$. This means that, in a numerical solution of equation (21), the integration has to include only a small section of the total space adjacent to the maximum of G_U ($G_{\underline{U}} \neq 0$).

$T_3 \rightarrow T_1$ and $c_{3,i} \rightarrow c_{1,i}$ form the new profiles to start the iteration with a further increment Δt according to equations (32) - (35) by including contributions of the chemical reaction terms. Steps 2 and 3 are repeated iteratively. Step 1 can be included as often as new hot spots occur from an external heat source, but this is not the case here.

Summing up all lattice nodes, where conversion is complete, defines a conversion rate, which in a linear progression can be considered as a burning rate.

The calculations result in three-dimensional temperature and concentration profiles for each time increment, and in the heat output and position of the reaction front over time; the plots are mainly two-dimensional cross sections

of these profiles.

The model does not include any convection or radiation. Finally, three types of parameters are necessary to run the Hot-Spot model in the version described:

- Initial distributions of fuel (or oxidizer) particles, an initiating temperature profile *e.g.* one or more Hot Spots.
- Material parameters: density, heat capacity, heat conductivity, diffusion coefficients for the species.
- Reaction parameters: heats of reactions, Arrhenius parameters (pre-exponential factors, activation energies).

Results of Hot-Spot calculations

The aim of the actual calculations was the simulation of the influence of the size of particles and the distance between them on the combustion behaviour in a cloud. The first step was to establish a representative distribution of fuel droplets. We chose 10×10 droplets of equal size in a quadratic configuration with equal distances in the x- and y-directions. Although this is only a 2-dimensional distribution, the effects should be clearly visible, the graphical representation is much easier and the calculations were much less time consuming than for a real 3-dimensional distribution. Ignition was simulated by a single hot-spot located either at the lower left hand corner of the droplet arrangement or in the centre of the droplet cloud. Material and reaction parameters were chosen to form a running system. In each series of calculations, the distance between the particles was varied and expressed as the l/d ratio. Figure 3 shows the development of the temperature profiles of the first series of calculations, with ignition at the lower left hand corner of the ensemble, after specific time intervals. Calculations were done for l/d ratios of: 0.5, 0.8, 1.0, 1.2, 1.5, 1.6, 1.7, 1.8, 1.9, 2.0, 2.2, 2.3, 2.4, and 2.5. Figure 3 presents the results for ratios of 0.5, 1.2, 1.6, 2.0, and 2.4. At the lowest l/d ratio, essentially no reaction occurs inside the cloud, but the reaction starts at the ignition point and propagates around the border of the ensemble. With increasing distance between the fuel droplets, which corresponds with an increasing amount of oxidizer between the droplets, reaction inside the cloud occurs. At an l/d ratio greater than 2, the fuel inside the cloud is completely consumed. With an l/d ratio greater than 2.4, the distance between the droplets becomes too large for propagation of the reaction.

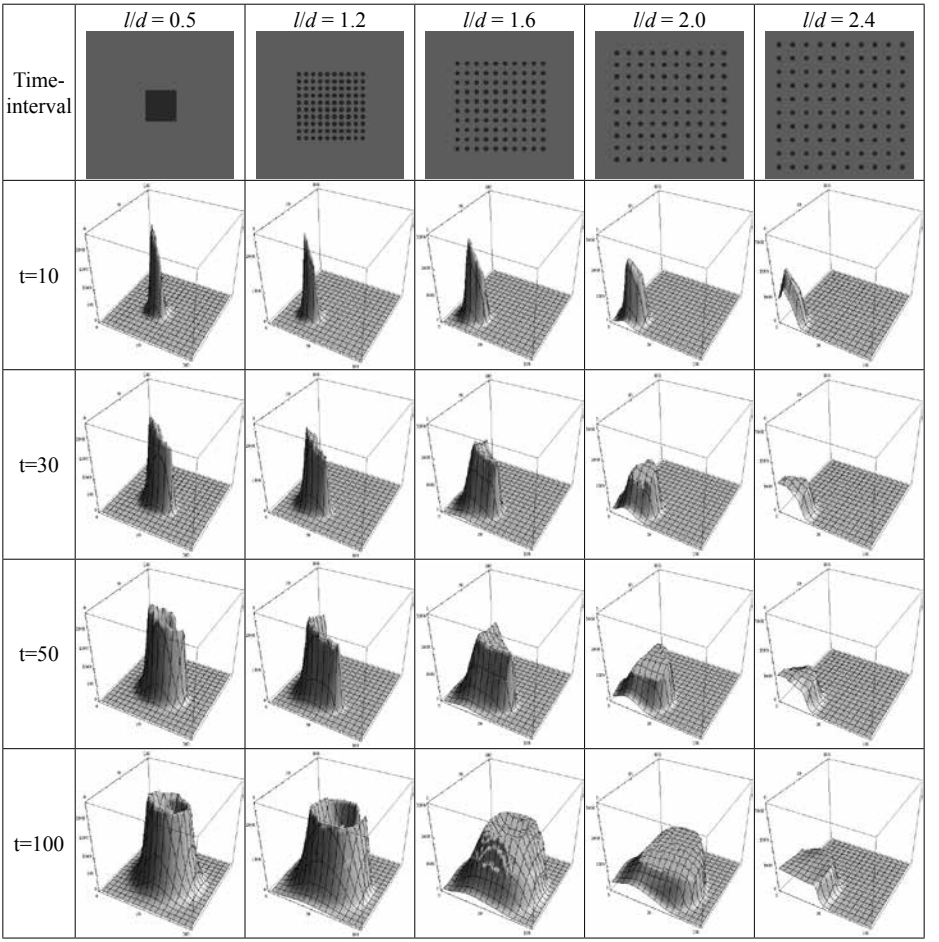

Figure 3. Development of temperature profiles after a certain number of time increments for *l*/*d* ratios = 0.5, 1.2, 1.6, 2.0 and 2.4, ignition at the lower left hand corner of the ensemble.

In a second series of calculations, the ignition position was changed to the center of the cloud. Figure 4 shows the temperature profiles resulting from these calculations. The main difference is that the reaction cannot propagate before an *l*/*d* ratio greater 1.4 is reached, because of the lack of oxidizer inside the cloud. On the other hand, the reaction can also run at *l*/*d* ratios greater than 2.4. The maximum distance for this configuration was 2.7.

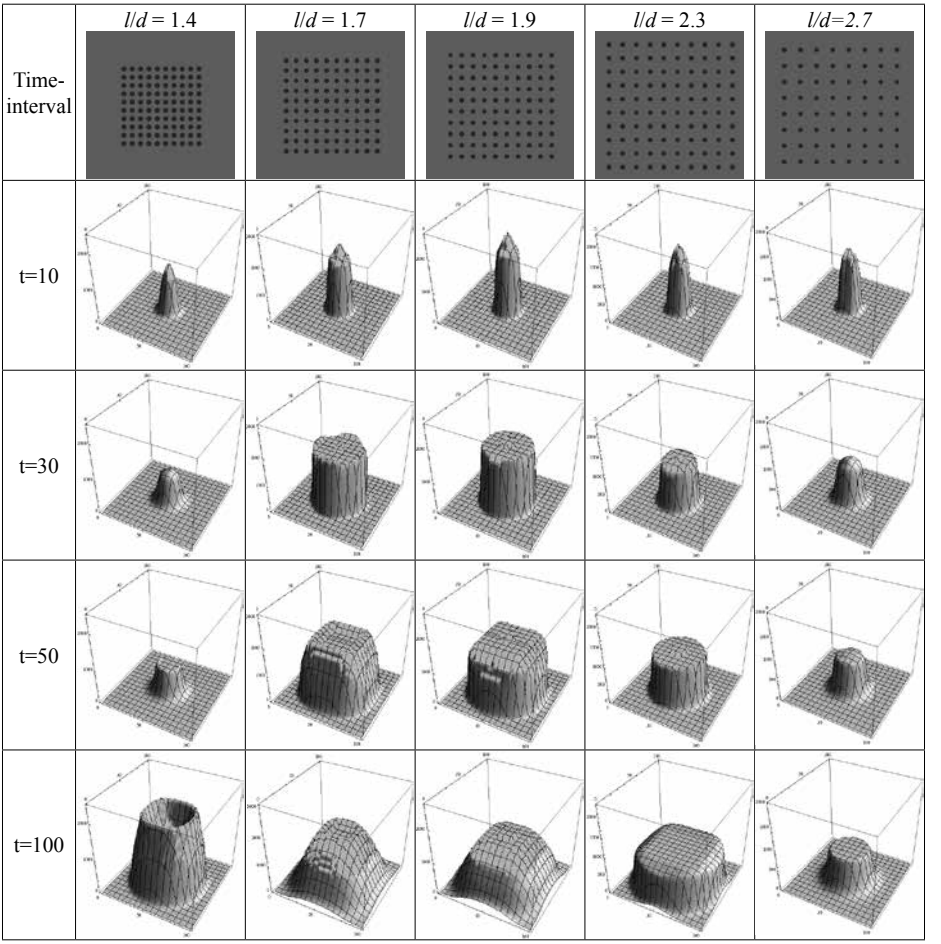

Figure 4. Development of temperature profiles after certain number of time increments for *l*/*d* ratios = 1.4, 1.7, 1.9, 2.3 and 2.7, ignition at the center of the ensemble.

Discussion and Conclusions

A comparison of the results of the quasi steady-state theory and the Hot-Spot-Model shows that they describe the same phenomenon of a common flame front for droplet clouds with a high density of droplets. But the Hot-Spot-Model can show more detail because of its transient nature. In the literature [22, 23], a phenomenological classification has been described, which distinguishes

between four burning regions: external sheath combustion, external group combustion, internal group combustion and single droplet combustion. In our Hot-Spot calculations we could see only two of these, external sheath combustion and single droplet combustion. The reason for this is the statistical nature of a real droplet cloud. In our calculations we tried a regular distribution first. In statistically distributed droplets, the distance between the droplets varies. Therefore, zones of higher and lower droplet concentrations can exist, which can react in different ways resulting in the two burning regions of group combustion. With statistical distribution the Hot-Spot-Model can perhaps show these phenomena. As no phase transitions are considered, the process of evaporation within the cloud cannot be simulated. The explicit representation for the burning of isolated droplets and their progression in a cloud needs more finely tuned parameters, work which will be attempted in the future. It will also include the use of realistic parameters.

References

[1] Wen D., Nanofuel as a Potential Secondary Energy Carrier, *Energy Environ. Sci.*, **2010**, *3*, 591-60.

[2] Tulis A.J., Sumida W.K., Dillon J., Comeyne W., Heberlein D.C., Submicron Aluminum Particle Size Influence on Detonation of Dispersed Fuel-oxidizer Powders, *Arch. Comb.*, **1998**, *18*(1-4), 157-164.

[3] Pritchard D.K., *Literature Review – Explosion Hazards Associated with Nanopowders*, HSL/2004/12, Health and Safety Laboratory, Buxton, **2004**.

[4] Dobashi R., Risk of Dust Explosions of Combustible Nanomaterials, Nanosafe 2008: International Conference on Safe production and use of nanomaterials, *Journal of Physics: Conference Series*, **2009**, *170*, 012029.

[5] Wu H.-C., Chang R.-C., Hsiao H.-C., Research of Minimum Ignition Energy for Nano Titanium Powder and Nano Iron Powder, *Journal of Loss Prevention in the Process Industries*, **2009**, *22*, 21-24.

[6] Wu H.-C., Ou H.-J., Peng D.-J., Hsiao H.-C., Gau C.-Y., Shih T.-S., Dust Explosion Characteristics of Agglomerated 35nm and 100nm Aluminum Particles, Hindawi Publishing Corporation, *Int. J. Chem. Eng.*, Article ID 941349, **2010**.

[7] Dufaud O., Traoré M., Perrin L., Chazelet S., Thomas D., Experimental Investigation and Modelling of Aluminum Dusts Explosions in the 20 L Sphere, *J. Loss. Prev. Process Ind.*, **2010**, *23*, 226-236.

[8] Andrzejak T.A., Shafirovich E., Varma A., On the Mechanisms of Titanium Particle Reactions in O2/N2 and O2/Ar Atmospheres, *Propellants Explos. Pyrotech.*, **2009**, *34*, 53-58.

[9] Meinkohn D., The Effect of Particle Size and Ambient Oxidizer Concentration on

Metal Particle Ignition, *Combust. Sci. Technol.*, **2009**, *181*(4), 1007-1037.
[10] Joyce D.M., *Combustion Signatures of Various Energetic Metal Powders in a Shock Tube Experiment*, Thesis, University of Illinois at Urbana-Champaign, **2011**.
[11] Marion M., Chauveau C., Gökalp I., Studies on the Ignition and Burning of Levitated Aluminum Particles, *Combust. Sci. Technol.*, **1996**, *115*, 369-390,.
[12] Natan B., Gany A., Ignition and Combustion of Boron Particles in the Flow Field of a Solid Fuel Ramjet, *J. Propul. Power*, **1991**, 7, 37-43.
[13] Zhow W., Yetter R.A., Dryer F.L., Rabitz H., Brown R.C., Kolb C.E., Multi-Phase Model for Ignition and Combustion of Boron Particles, *Combust. Flame*, **1999**, *117*(1), 227-243.
[14] Dirk Meinkohn, The Effect of Particle Size and Ambient Oxidizer Concentration on Metal Particle Ignition, *Combust. Sci. Technol.*, **2009**, *181*(4), 1007-1037.
[15] Umemura A., Ogawa S., Oshima N., Analysis of the Interaction between Two Burning Droplets, *Combust. Flame*, **1981**, *41*, 45-55.
[16] Marberry M., Ray A.K., Leung K., Effect of Multiple Particle Interactions on Burning Droplets, *Combust. Flame*, **1984**, *57*(3), 237-245.
[17] Miyasaka K., Law C.K., Combustion of Strongly-Interacting Linear Droplet Arrays, *18th Symp. (Int.) Combust.*, **1981**, 283.
[18] Xiong T.Y., Law C.K., Miyasaka K., Interactive Vaporization and Combustion of Binary Droplet Systems, *20th Symp. (Int.) Combust.*, **1985**, 1781-1787.
[19] Nagata H., Kudo I., Ito K., Nakamura S., Takeshita Y., Interactive Combustion of Two-Dimensionally Arranged Quasi-Droplet Clusters under Microgravity, *Combust. Flame*, **2002**, *129*, 392-400.
[20] Abramzon B., Sirignano W.A., Droplet Vaporization Model for Spray Combustion Calculations, *Int. J. Heat. Mass Transfer*, **1989**, *32*(9), 1605-1618.
[21] Kim H.Y., Cho C.P., Chung J.T., Correlation of Burning Rate of the Interacting Liquid Droplets with Internal Circulation, *JSME International Journal Series B*, **2005**, *48*(2), 293-299.
[22] Chin H.H., Kim H.Y., Croke E.J., Internal Group Combustion of Liquid Droplets, *19th Symp. (Int.) Combust.*, The Combustion Institute, Pittsburgh, PA, **1983**, 971-80.
[23] Correa S. M., Sichel M., The Group Combustion of a Spherical Cloud of Monodisperse Fuel Droplets, *19th Symp. (Int.) Combust.*, The Combustion Institute, Pittsburgh, PA, **1983**, 981-91.
[24] Law C.K., Surface Reaction Model for Metal Particle Combustion, *Combust. Sci. Technol.*, **1973**, 7, 197-212.
[25] Eisenreich N., Borne L., Lee R.S., Forbes J.W., Ciezki H.K., Particle Processing and Characterization, ch. 13, in: *Energetic Materials* (U. Teipel, Ed.), Wiley-VCH, **2005**.
[26] Ilyin A.P., Proskurovskaya L.T., Two Stage Combustion of Ultradispersed Aluminum Powder in Air, *Combust., Explos. Shock Waves (Eng. Transl.)*, **1990**, *26*(2), 71-72.
[27] Mench M.M., Yeh C.L., Kuo K.K., Propellant Burning Rate Enhancement and Thermal Behavior of Ultra-Fine Aluminum Powders (ALEX), *29th Int. Annu. Conf.*

ICT , June 30-July 3, **1998**, 30(1-15).

[28] Bashung B., Grune D., Licht H.H., Samirant M., Combustion Phenomena of a Solid Propellant Based on Aluminum Powder, *5th International Symposium on Special Topics in Chemical Propulsion (5-ISICP)*, Stresa, Italy, 19-22 June, **2000**.

[29] Lessard P., Beaupré F., Brousseau P., Burn Rate Studies of Composite Propellants Containing Ultra-Fine Metals, *32nd Int. Annu. Conf. ICT*, Karlsruhe, 3-6 July, **2001**.

[30] Weiser V., Eisenreich N., Kelzenberg S., Einfluß der Größe von Metallpartikeln auf die Anzündung und Verbrennung von Energetischen Materialien, *32nd Int. Annu. Conf. ICT*, Karlsruhe, Germany, **2001**, July 3 – July 6, 34.1-34-14.

[31] Arkhipov V., Bondarchuk S., Vorozhtsov A., Korotkikh A., Kuznetsov V., Ivanov Yu.F., Osmonoliev M.N., Sedoi V.S., Productions of Ultra-Fine Powders and Their Use in High Energetic Compositions, *Propellants Explos. Pyrotech.*, **2003**, *28*, 319-333.

[32] Vorozhtsov A., Arkhipov V., Bondarchuk S., Kuznetsov V., Korotkikh A., Surkov V., Ignition and Combustion of Solid Propellants Containing Ultrafine Aluminum, *Proc. Rocket Propulsion: Present and Future*, Pozzuoli, Naples, Italy, 16-21 June, **2002**, 8-IWCP Book of Abstracts, Politecnico di Milano, SP Lab, Printed in Italy, **2002**, 78-79.

[33] Simonenko V.N., Zarko V.E., Comparative Studying the Combustion Behavior of Fine Aluminum, *30th Int. Annu. Conf. of ICT*, Karlsruhe, June 29 – July 2, **1999**, 21(1-14).

[34] Miller P.J., Bedford C.D., Davis J.J., Effect of Metal Particle Size on the Detonation Properties of Various Metallized Explosives, *11th Int. Symposium on Detonation, Snowmass*, Colorado, 30 August – 4 September, **1998**.

[35] Lefrançois A., LeGallic C., Expertise of Nanometric Aluminum Powder on the Detonation Efficiency of Explosives, *32nd Int. Annu. Conf. ICT*, Karlsruhe, Germany, 3-6 July, **2001**.

[36] Brousseau P., Cliff M.D., The Effect of Ultrafine Aluminium Powder on the Detonation Properties of Various Explosives, *32nd Int. Annu. Conf. ICT*, Karlsruhe, Germany, 3-6 July, **2001**.

[37] Liu Q., Bai C., Jiang L., Dai W., Deflagration-to-Detonation Transition in Nitromethane Mist/Aluminum Dust/Air Mixtures, *Combust. Flame*, **2010**, *157*, 106-117.

[38] Eisenreich N., Fietzek H., Juez-Lorenzo M., Kolarik V., Koleczko A., Weiser V., On the Mechanism of Low Temperature Oxidation for Aluminium Particles down to the Nano-Scale, *Propellants Explos. Pyrotech.*, **2004**, *29*, 137-145.

[39] Trunov M.A., Schoenitz M., Dreizin E.L., Ignition of Aluminum Powders under Different Experimental Conditions, *Propellants Explos. Pyrotech.*, **2005**, *30*, 36.

[40] Trunov M.A., Umbrajkar S.M., Schoenitz M., Mang J.T., Dreizin E.L., Oxidation and Melting of Aluminum Nanopowders, *J. Phys. Chem. B*, **2006**, *110*, 13094-13099.

[41] Schulz O., Eisenreich N., Kelzenberg S., Schuppler H., Neutz J., Kondratenko E., Non-isothermal and Isothermal Kinetics of High Temperature Oxidation of Micrometer-

Sized Titanium Particles in Air, *Thermochim. Acta*, **2011**, *517*, 98-104.
[42] Schulz O., Eisenreich N., Kelzenberg S., Fietzek H., Juez-Lorenzo M., Kondratenko E., Oxidation of Nanometer-Sized Titanium Nitride and Micrometer-Sized Titanium Particles with Titanium Nitride Traces up to 1473 K in Air, *Particle & Particle Systems Characterization*, **2010**, 7, 48-58.
[43] Langer G., Eisenreich N., Hot Spots in Energetic Materials, *Propellants Explos. Pyrotech.*, **1999**, *24*, 113-118.
[44] Weiser V., Kelzenberg S., Eisenreich N., Influence of Metal Particle Size on the Ignition of Energetic Materials, *Propellants Explos. Pyrotech.*, **2001**, *26*, 284-289.
[45] Eisenreich N., Fischer T.S., Langer G., Kelzenberg S., Weiser V., Burn Rate Models for Gun Propellants, *Propellants Explos. Pyrotech.*, **2002**, *27*, 142-149.
[46] Kelzenberg S., Eisenreich N., Weiser V., New Approach to Ignition and Combustion Phenomena with Hot-Spot-Model, Proc. *Theory and Practice of Energetic Materials*, Vol.VI, Beijing, China, October 25 – 28, Science Press USA Inc., **2005**, 803-809.
[47] Kelzenberg S., Eisenreich N., Weiser V., Fast Methods on Modelling of Multidimensional Distributions of Evaporating and Burning Droplets, *34th Int. Annu. Conf. ICT*, Karlsruhe, June 24 – 27, **2003**.
[48] Kelzenberg S., Eisenreich N., Modelling of Combustion of Droplet Cluster, *35th Int. Annu. Conf. ICT*, Karlsruhe, June 29 – July 2, P160, **2004**.
[49] Williams F.A., *Combustion Theory*, 2nd Edition, Benjamin/Cummings Publishing Company, Inc., **1985**.
[50] *Recent Advances in Spray Combustion*, (Kuo K.K., Ed.), Vol. I: Spray Atomization and Drop Burning Phenomena, Volume 166 of Progress in Astronautics and Aeronautics, AIAA, **1996**.
[51] Sirignano W.A., *Fluid Dynamics and Transport of Droplets and Sprays*, Cambridge University Press, UK, **1999**.
[52] Spalding D.B., *Combustion and Mass Transfer*, Pergamon Press, **1979**.
[53] Carslaw H.S., Jaeger J.C., *Conduction of Heat in Solids*, 2nd ed., Clarendon Press, Oxford, UK, **1973**.
[54] Press W.H., Flannery B.P., Teukolsky S.A., Vetterling W.T., *Numerical Recipes*, Cambridge University Press, London, **1986**.